Resonance effects in the 5σ photoionization of CO

Maile E. Smith,[a] Diane L. Lynch, and Vincent McKoy
Arthur Amos Noyes Laboratory of Chemical Physics,[b] California Institute of Technology, Pasadena, California 91125

(Received 18 August 1986; accepted 27 August 1986)

We report vibrational branching ratios and vibrationally resolved photoelectron angular distributions for resonant photoionization of the 5σ level of CO leading to $X\,^2\Sigma^+ CO^+$. These results were obtained using frozen-core Hartree–Fock photoelectron continuum orbitals. These studies provide a clear quantitative picture of the role of the $k\sigma$ shape resonance in the observed non-Franck–Condon behavior and useful insight into the interplay between this shape resonance and a valence-like autoionizing resonance around 23 eV.

I. INTRODUCTION

Shape resonances are known to lead to several prominent and important features in molecular photoionization. Among these features are non-Franck–Condon vibrational branching ratios over a wide energy range around the resonance and photoelectron angular distributions which are vibrational state dependent.[1–8] These effects arise from the strong dependence of the dipole transition matrix element for photoionization on internuclear separation. Such non-Franck–Condon vibrational intensity distributions due to a shape resonance were first predicted by Dehmer *et al.*[3] for photoionization of the $3\sigma_g$ level of N_2 and confirmed experimentally for this same system by West *et al.*[2]

The studies of Dehmer *et al.*,[3] which used the continuum multiple scattering model, predicted larger deviations from Franck–Condon behavior than were observed experimentally.[2] The results of subsequent studies of these vibrational branching ratios using Hartree–Fock photoelectron continuum orbitals were in very good agreement with the measured data for photon energies away from known autoionizing features.[8] This result is not surprising since the Hartree–Fock model can be expected to work well for shape resonances which are, in fact, one electron in nature.

Non-Franck–Condon behavior has also been observed in both the vibrational intensities[4] and photoelectron angular distributions[5] for photoionization of the 5σ level of CO for photon energies between 16 and 27 eV. Although the σ shape resonance in the photoionization continuum of CO, in analogy to the $3\sigma_g$ channel of N_2, should also contribute significantly to this non-Franck–Condon behavior, both the experimental data[4,5] and theoretical studies of these vibrational intensities and angular distributions[9] suggest that this behavior arises from a more subtle and physically important interplay between shape and autoionizing resonances in CO than in N_2. The difference in the non-Franck–Condon behavior around the shape resonance in N_2 and CO arises from the observation that, whereas in N_2 the peak of the $3\sigma_g \rightarrow k\sigma_u$ shape resonance lies at 5 eV above the doubly excited autoionizing state at 23 eV, in CO the maximum of the shape resonance and the autoionizing state are within about 1.5 eV of each other. Since both the shape and autoionizing resonances lead to non-Franck–Condon behavior, some important differences can be expected in the vibrational intensities and related angular distributions in these two systems. In fact, Stephens *et al.*[9] have used the continuum multiple scattering model to obtain the non-Franck–Condon behavior due to the shape resonance in the 5σ photoionization of CO. The significant discrepancies between the results of these calculations and the experimental data, particularly for the higher vibrational levels, were attributed to an autoionizing resonance.

In this paper we report vibrational branching ratios and photoelectron asymmetry parameters for shape resonant photoionization of the 5σ level of CO. These studies are carried out using Hartree–Fock continuum states for the photoelectron orbital and, hence, should adequately account for the non-Franck–Condon behavior of the branching ratios and asymmetry parameters arising from the shape resonance. Such information is an important first step towards understanding the role of the autoionizing resonance in the observed photoionization cross sections. We will see, in fact, that our calculated branching ratios for the $v' = 1$ and 2 levels, are quite different from those of the multiple scattering model and help to readily identify the autoionizing contributions to the experimentally observed structure. Further calculations are required to include the effect of the autoionizing resonance on the cross sections. Such studies are under way. We note, however, that the electronic configuration of this autoionizing resonance is not yet certain. Stephens *et al.*[9] have suggested the doubly excited configuration $5\sigma 1\pi^3 2\pi^2$. As we will see, if this is the correct electronic configuration, the autoionizing resonance will interact not with the σ shape resonant continuum but with the nonresonant π background.

The outline of the paper is as follows. In the next section we present some relevant details of our procedure for obtaining the photoionization matrix elements and of the potential energy curves used. We then compare the resulting vibrational branching ratios and photoelectron angular distributions for $v' = 0,1$, and 2 with the available experimental data and with the results of calculations using the multiple scattering model.

[a] Present address: Institute for Defense Analyses, Science and Technology Division, 1801 North Beauregard Street, Alexandria, VA 22311.
[b] Contribution No. 7435.

 0021-9606/86/236455-05$02.10

II. METHOD AND CALCULATIONS

In our calculations of the photoionization cross sections we use a Hartree–Fock wave function for the initial state. For the final photoionized state we use a frozen-core Hartree–Fock model in which the bound orbitals are assumed identical to those in the initial state Hartree–Fock wave function and the photoelectron continuum orbital is determined in the field of these $(N-1)$ unrelaxed core orbitals. The Hartree–Fock photoelectron continuum orbitals then satisfy a one-electron Schrödinger equation

$$(-\tfrac{1}{2}\nabla^2 + V_{N-1}(\mathbf{r},R) - k^2/2)\phi_{\mathbf{k}}(\mathbf{r},R) = 0, \tag{1}$$

where $k^2/2$ is the photoelectron kinetic energy and $\phi_{\mathbf{k}}$ satisfies the appropriate boundary conditions. If we expand this continuum orbital $\phi_{\mathbf{k}}$ in spherical harmonics defined about the direction of $\mathbf{k}$, i.e.,

$$\phi_{\mathbf{k}}(\mathbf{r},R) = \left(\frac{2}{\pi}\right)^{1/2} \sum_{lm} i^l \psi_{klm}(\mathbf{r},R) Y^*_{lm}(\hat{k}), \tag{2}$$

the functions $\psi_{klm}(\mathbf{r},R)$ satisfy the same Schrödinger equation as $\phi_{\mathbf{k}}$ itself. With these functions $\psi_{klm}(\mathbf{r},R)$ we define the length and velocity forms of the photoionization transition matrix element as

$$I^L_{lm\mu}(R) = k^{1/2}\langle \phi_{5\sigma}(\mathbf{r},R)|r_\mu|\psi_{klm}(\mathbf{r},R)\rangle \tag{3}$$

and

$$I^V_{lm\mu}(R) = \frac{k^{1/2}}{E}\langle \phi_{5\sigma}(\mathbf{r},R)|\nabla_\mu|\psi_{klm}(\mathbf{r},R)\rangle, \tag{4}$$

where $\phi_{5\sigma}$ is the occupied 5σ orbital of CO and E is the photon energy. In terms of these matrix elements $I^{L,V}_{lm\mu}$ the cross section for photoionization of the 5σ orbital out of the $\nu = 0$ vibrational level of the ground state and into the $\nu' = n$ level of CO^+ can be written as

$$\sigma^{L,V}_{\nu=0,\nu'=n} = \frac{4\pi^2}{3c} E \sum_{lm\mu} |\langle \chi_i^{\nu=0}(R)|I^{L,V}_{lm\mu}|\chi_f^{\nu'=n}(R)\rangle|^2, \tag{5}$$

where the χ's are vibrational wave functions and c is the speed of light.

The corresponding photoelectron asymmetry parameter is defined as

$$\frac{d\sigma^{L,V}_{\nu=0,\nu'=n}}{d\Omega_{\hat{k}}} = \frac{\sigma^{L,V}_{\nu=0,\nu'=n}}{4\pi}\left[1 + \beta^{L,V}_{k,\nu=0,\nu'=n} P_2(\cos\theta)\right], \tag{6}$$

where θ is the angle between the direction of polarization of the light and the momentum of the electron.

To obtain the photoelectron continuum orbital ψ_{klm}, which satisfies the Schrödinger equation of Eq. (1), ψ_{klm} is further expanded in partial waves. The resulting coupled equations are solved using an adaptation of the Schwinger variational principle for long-range potentials in which the static component of the electron–molecule interaction is treated exactly by numerical integration and the exchange interactions are approximated by a separable potential of the Schwinger type.[10] This method,[10] which leads to variationally stable scattering matrices and photoionization cross sections at the Hartree–Fock level, has been shown to be effective for obtaining electronic continuum solutions of strongly polar ions such as $CO^+[5\sigma^{-1}]$. Furthermore, the method also includes an iterative procedure for obtaining the converged scattering solutions. Details of this approach are discussed in Ref. 10. In these studies we used the same partial wave expansions as those assumed by Lucchese and McKoy[11] in their vibrationally unresolved studies of the 5σ photoionization of CO. These expansion parameters should provide converged cross sections.

The photoelectron transition matrix element $I_{lm\mu}(R)$ of Eqs. (3) and (4) were evaluated at the five internuclear separations of $R = 1.898$, 2.015, 2.132, 2.249, and 2.366 a.u., where the equilibrium internuclear distance of CO is 2.132 a.u. At each internuclear distance we used the SCF wave function of McLean and Yoshimine.[12] In this wave function the molecular orbitals are expanded in Slater-type functions. The initial basis set used in the solution of the Lippmann–Schwinger equation associated with the Schrödinger equation, Eq. (1), contained seven Cartesian Gaussian functions defined by

$$\phi_{lmn}(\mathbf{r}) = N_{lmn}(x-A_x)^l(y-A_y)^m(z-A_z)^n \times \exp(-\alpha|\mathbf{r}-\mathbf{A}|^2). \tag{7}$$

These basis functions are specified in Table I. To ensure convergence of the photoionization cross sections, we evaluated the matrix element in Eq. (3) using photoelectron orbitals obtained after one step in our iterative procedure for solving the Lippmann–Schwinger equation.[10]

The vibrational wave functions were obtained from numerical solution of the Schrödinger equation using RKR potentials. We have outlined this method in our earlier studies of N_2.[8] For CO and CO^+ we used the RKR curves of Tobias *et al.*[13] ($R_e = 1.128$ Å) and Singh and Rai[14] ($R_e = 1.115$ Å), respectively. With this approach we obtained the following Franck–Condon factors (FCF): $(\nu=0,\nu'=0) = 0.9607$, $(\nu=0,\nu'=1) = 0.0391$, and $(\nu=0,\nu'=2) = 0.000\,152$. These values agree quite well with the FCF's obtained previously by Albritton[15] [$(\nu=0,\nu'=1) = 0.038$] and Wacks[16] [$(\nu=0,\nu'=0) = 0.9636$, $(\nu=0,\nu'=1) = 0.036\,34$, $(\nu=0,\nu'=2) = 0.000\,11$].

III. RESULTS AND DISCUSSION

Figure 1 shows the fixed-nuclei cross sections for photoionization out of the 5σ orbital of CO at five internuclear

TABLE I. Initial scattering basis sets used in obtaining the σ and π photoelectron orbitals.[a]

	Center	l	m	n	α
$5\sigma \to k\sigma$	C	0	0	0	10.0,4.0,1.5,0.5,0.1
	C	0	0	1	1.0,0.1
	O	0	0	0	10.0,4.0,1.5,0.5,0.1
	O	0	0	1	1.0,0.1
$5\sigma \to k\pi$	C	1	0	0	10.0,4.0,1.5,0.5,0.1
	C	1	0	1	1.0,0.1
	O	1	0	0	10.0,4.0,1.5,0.5,0.1
	O	1	0	1	1.0,0.1

[a] See Eq. (7) in the text.

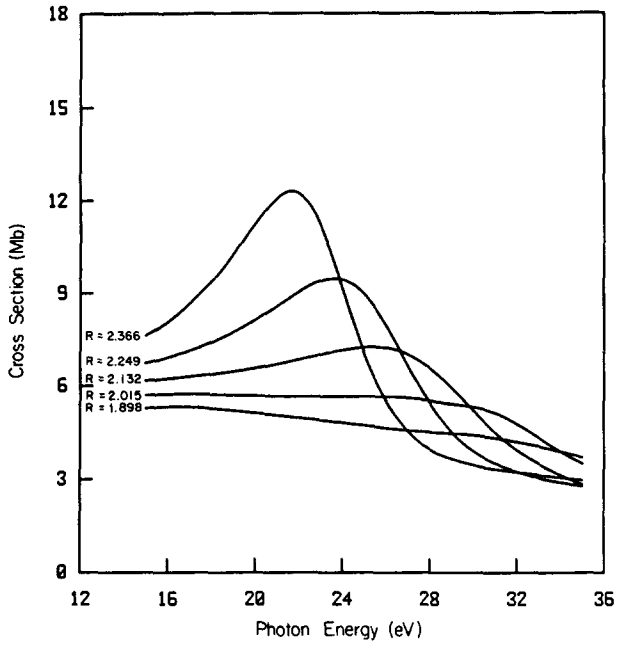

FIG. 1. Fixed-nuclei photoionization cross sections (dipole length) for the 5σ level of CO at five internuclear distances.

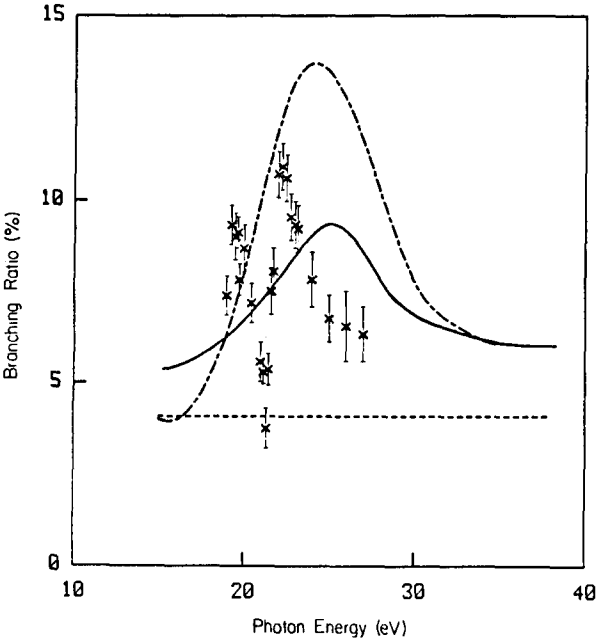

FIG. 3. Branching ratio for the $v' = 1$ level of CO^+ $X^2\Sigma^+$:—, present results (dipole length); – – –, multiple scattering model (Ref. 9); ×, experimental results (Ref. 4); – – –, Franck–Condon values.

distances. The photon energy scale here assumes an ionization potential of 14.0 eV. For reasons that are well understood, the resonance broadens and shifts to higher energy as the internuclear distance decreases. It is this dependence of the cross section on internuclear distance that leads to non-Franck–Condon behavior in the vibrational state distributions and photoelectron angular distributions.

In Fig. 2 we show the vibrationally resolved 5σ cross sections for the $v' = 0$, $v' = 1$, and $v' = 2$ levels. It is worth noting that although the resonances in $v' = 1$ and 2 are shifted to higher energy than in $v' = 0$, the shift in going from $v' = 0$ to $v' = 1$ is smaller than in N_2.[4,8] In this figure the cross sections for $v' = 1$ and 2 are actually scaled up by factors of 10 and 100, respectively. The vibrational branching ratios for photoionization into the $v' = 1$ and $v' = 2$ levels, expressed as a percentage of the $v' = 0$ level, are shown in Figs. 3 and 4 along with the predictions of the multiple scattering model[9] and the experimental data of Stockbauer *et al.*[4] The horizontal dashed lines in these figures represent the

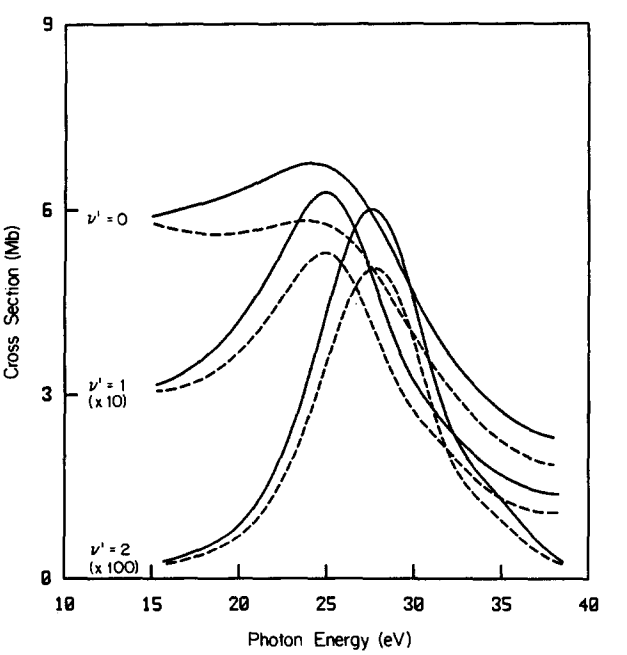

FIG. 2. Vibrationally resolved photoionization cross sections for the $v' = 0,1$, and 2 levels of the $X^2\Sigma^+(5\sigma^{-1})$ state of CO^+:—, dipole length; – – –, dipole velocity.

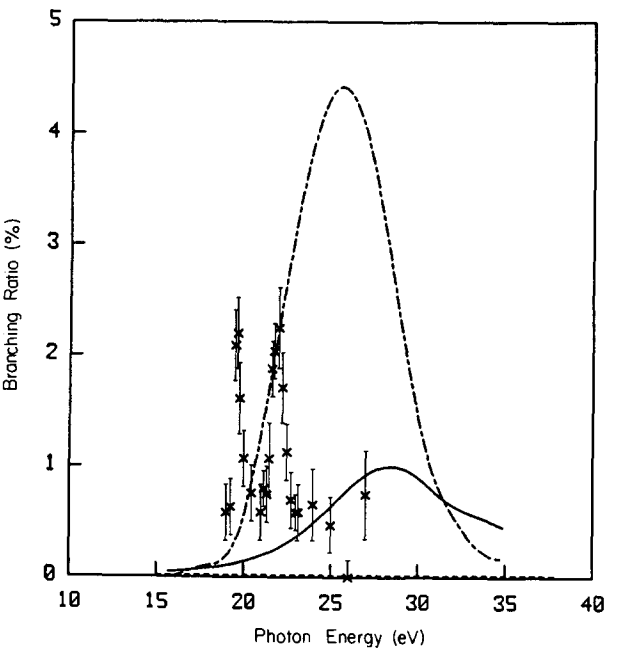

FIG. 4. Branching ratio for the $v' = 2$ level of CO^+ $X^2\Sigma^+$:—, present results (dipole length); – – –, multiple scattering model (Ref. 9); ×, experimental results (Ref. 4); – – –, Franck–Condon values.

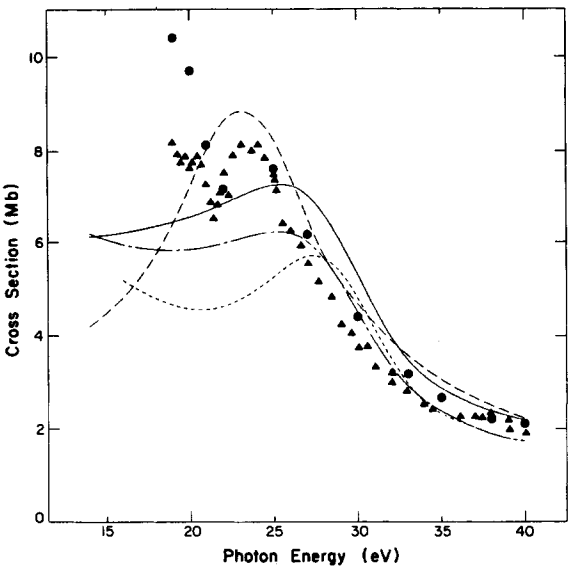

FIG. 5. Vibrationally unresolved photoionization cross sections for the $X\,^2\Sigma^+(5\sigma^{-1})$ level of CO^+: —, present results (dipole length), – – –, present results (dipole velocity); - - -, multiple scattering model (Ref. 17); – – –, Stieltjes–Tchebycheff moment theory (Ref. 18); ●, experimental data (Ref. 19); ▲, experimental data (Ref. 20). (See Ref. 11 for further details of this figure.)

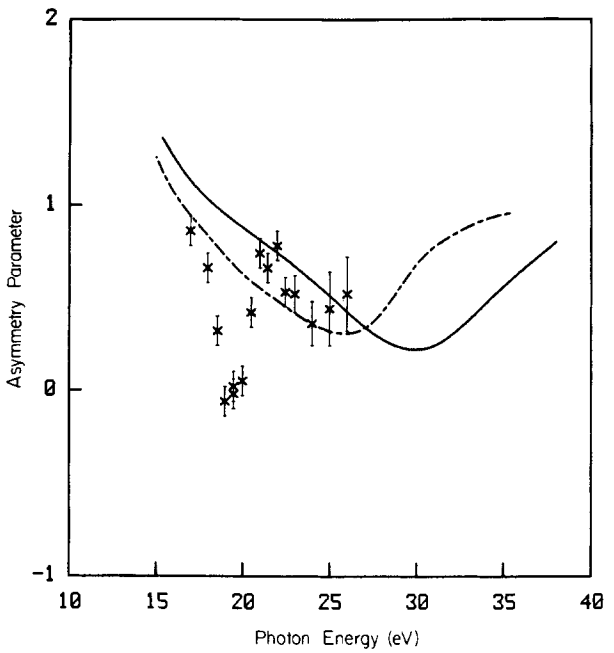

FIG. 7. Photoelectron asymmetry parameters for the $v' = 1$ level of CO^+ $X\,^2\Sigma^+$: —, present results (dipole length); – – –, multiple scattering model (Ref. 9); ×, measured values (Ref. 5).

Franck–Condon values of the branching ratios.

A comparison of our calculated branching ratios and the measured values shows that structure due to the autoionizing resonance distinctly dominates the observed branching ratios over this range of photon energies. The enhancement in the branching ratios centered around 19.5 eV has been attributed to unresolved autoionization structure associated with the CO^+ $B\,^2\Sigma^+$ state at 19.7 eV.[5] The structure broadly centered around 23 eV is not well understood but has been suggested[9] to arise from autoionization of the valence-like state with a possible electron configuration of $\ldots 4\sigma^2 5\sigma 1\pi^3 2\pi^2$. This autoionizing feature is also very apparent in a comparison of calculated vibrationally unresolved photoionization cross sections with the experimental data.[11] These results, which are taken from an earlier publication,[11] are shown in Fig. 5 for convenience. In this figure the feature appears as a broad hump between about 21 and 25 eV lying

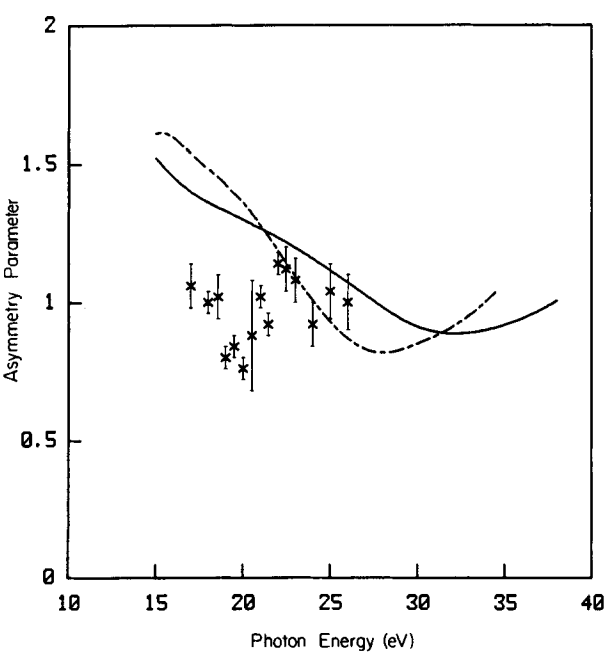

FIG. 6. Photoelectron asymmetry parameters for the $v' = 0$ level of CO^+ $X\,^2\Sigma^+$: —, present results (dipole length); – – –, multiple scattering model (Ref. 9); ×, measured values (Ref. 5).

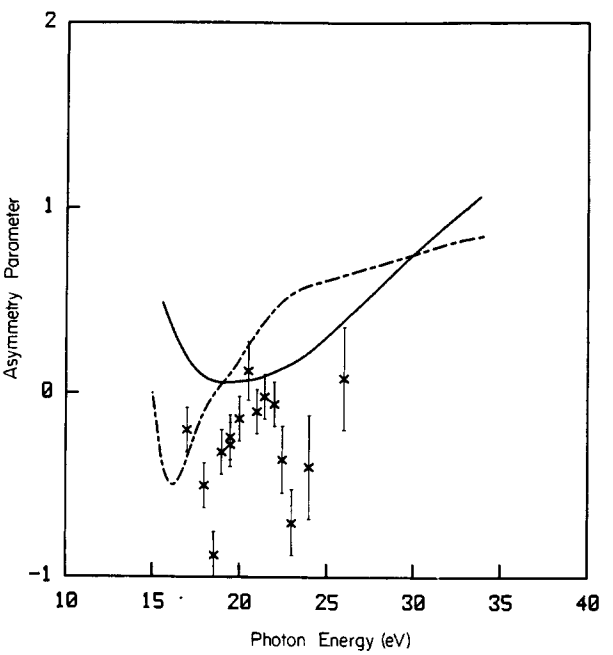

FIG. 8. Photoelectron asymmetry parameters for the $v' = 2$ level of CO^+ $X\,^2\Sigma^+$: —, present results (dipole length): – – –, multiple scattering model (Ref. 9), ×, measured values (Ref. 5).

on a slowly varying shape resonant background. The branching ratios in Figs. 2 and 3 also indicate that this autoionizing state influences the branching ratios over a similar energy range and beyond. Again, this behavior is consistent with a valence-like resonance in this region which would be expected to affect the branching ratios over a wider energy range than a sharp Rydberg-like autoionizing state. This may be the reason for the differences between the calculated and measured $\nu' = 1/\nu' = 0$ branching ratios around 27 eV and, possibly, above. The trend in the measured $\nu' = 2/\nu' = 0$ branching ratios at 27 eV, and its similarity to the calculated shape-resonant values, suggests that it is beyond this energy that the branching ratios will be dominated by the shape resonance. Measurements of these branching ratios at higher photon energies are clearly needed. It is worth noting that if the autoionizing state around 23 eV does have the electron configuration $...4\sigma^2 5\sigma 1\pi^3 2\pi^2$, such a resonance will couple with the non-shape-resonant $^1\Pi$ background continuum and not with the $k\sigma$ shape resonant continuum. Finally, comparison of the branching ratios obtained from the multiple scattering model[9] with the present results and the measured ratios shows that this model overestimates the magnitude of the non-Franck–Condon behavior arising from the shape resonance but certainly illustrates the underlying feature.

The occurrence of non-Franck–Condon behavior due to overlapping of a shape and autoionizing resonance in the $\nu' = 1/\nu' = 0$ branching ratios of CO^+ in Fig. 3 differs significantly from what was seen in earlier studies of the photoionization of $N_2(3\sigma_g^{-1})$. As discussed by Stephens *et al.*,[9] and seen very clearly in recent measurements of the photoelectron asymmetry parameters of $N_2^+(3\sigma_g^{-1})X\,^2\Sigma_g^+$, $\nu' = 0$,[21] although the autoionizing resonance also occurs around 23 eV in N_2, the shape-resonant non-Franck–Condon behavior there has a maximum at about 34 eV, well removed from the 25 eV position in CO. It is also interesting to note that the suggested valence configuration[9,17] of $...1\pi_u^3 3\sigma_g 1\pi_g^2(^1\Pi_u)$ for this resonance in N_2 would be consistent with the known role of the core-excited $1\pi_u^3 3\sigma_g^2 1\pi_g^2(^2\Pi_u)$ shape resonance, with a $1\pi_u^3 3\sigma_g^2 1\pi_g(^3\Sigma_u)$ parent, in the electron impact excitation spectrum of N_2.[22]

Figures 6–8 show our calculated photoelectron asymmetry parameters for the $\nu' = 0$, 1, and 2 vibrational levels of $CO^+(X\,^2\Sigma^+)$ along with the experimental data of Cole *et al.*[5] and the results of the multiple scattering model.[9] The measured photoelectron asymmetry parameters are again dominated by structure due to the autoionizing resonances which appear as pronounced dips from the smooth background of the calculated values. The calculated asymmetry parameters show a minimum which becomes more developed and moves to lower energy with increasing ν'. The behavior in the calculated $\nu' = 0$ asymmetry parameters at higher energy, e.g., the shallow minimum around 32 eV, also agrees with the vibrationally unresolved measurements of Marr *et al.*,[23] reflecting the dominance of the $\nu = 0 \rightarrow \nu' = 0$ component. Measurements of these asymmetry parameters for the $\nu' = 1$ and $\nu' = 2$ levels at higher photon energies, i.e., beyond 27 eV, would provide a useful check of the predicted behavior in Figs. 7 and 8.

ACKNOWLEDGMENT

This material is based upon research supported by the National Science Foundation under Grant No. CHE-8521391.

[1] J. L. Dehmer, D. Dill, and A. C. Parr, in *Photophysics and Photochemistry in the Vacuum Ultraviolet,* edited by S. P. McGlynn *et al.* (Reidel, Dordrecht, 1985), pp. 341–408.
[2] J. B. West, A. C. Parr, B. E. Cole, D. L. Ederer, R. Stockbauer, and J. L. Dehmer, J. Phys. B **13**, L105 (1980).
[3] J. L. Dehmer, D. Dill, and S. Wallace, Phys. Rev. Lett. **43**, 1005 (1979).
[4] R. Stockbauer, B. E. Cole, D. L. Ederer, J. B. West, A. C. Parr, and J. L. Dehmer, Phys. Rev. Lett. **43**, 757 (1979).
[5] B. E. Cole, D. L. Ederer, R. Stockbauer, K. Codling, A. C. Parr, J. B. West, E. D. Poliakoff, and J. L. Dehmer, J. Chem. Phys. **72**, 6308 (1980).
[6] T. A. Carlson, M. O. Krause, D. Mehaffy, J. W. Taylor, F. A. Grimm, and J. D. Allen, Jr., J. Chem. Phys. **73**, 6056 (1980).
[7] P. R. Keller, D. Mehaffy, J. W. Taylor, F. A. Grimm, and T. A. Carlson, J. Electron. Spectrosc. Relat. Phenom. **27**, 223 (1982).
[8] R. R. Lucchese and V. McKoy, J. Phys. B **14**, L629 (1981).
[9] J. A. Stephens, D. Dill, and J. L. Dehmer, J. Phys. B **14**, 3911 (1981).
[10] M. E. Smith, R. R. Lucchese, and V. McKoy, Phys. Rev. A **29**, 1857 (1984).
[11] R. R. Lucchese and V. McKoy, Phys. Rev. A **28**, 1382 (1983).
[12] A. D. McLean and M. Yoshimine, *Tables of Linear Molecule Wave Functions* (IBM San Jose Research Laboratory, San Jose, CA, 1967).
[13] I. Tobias, R. J. Fallon, and J. T. Vanderslice, J. Chem. Phys. **33**, 1638 (1960).
[14] R. B. Singh and D. K. Rai, J. Mol. Spectrosc. **19**, 424 (1966).
[15] D. L. Albritton (quoted as a private communication in Ref. 9).
[16] M. Wacks, J. Chem. Phys. **41**, 930 (1964).
[17] J. W. Davenport, Phys. Rev. Lett. **36**, 945 (1976).
[18] N. Padial, G. Csanak, B. V. McKoy, and P. W. Langhoff, J. Chem. Phys. **69**, 2992 (1978).
[19] A. Hamnett, W. Stoll, and C. E. Brion, J. Electron Spectrosc. Relat. Phenom. **8**, 367 (1976).
[20] E. W. Plummer, T. Gustaffson, W. Gudat, and D. E. Eastman, Phys. Rev. A **15**, 2339 (1977).
[21] S. H. Southworth, A. C. Parr, J. E. Hardis, and J. L. Dehmer, Phys. Rev. A **33**, 1020 (1986).
[22] J. Mazeau, F. Gresteau, R. I. Hall, G. Joyez, and J. Reinhardt, J. Phys. B **6**, 862 (1973).
[23] G. V. Marr, J. M. Morton, R. M. Homes, and D. G. McCoy, J. Phys. B **12**, 43 (1979).